FOI-R--0300--SE

December 2001

ISSN 1650-1942

Methodology report

Inversion of seabed parameters in the Stockholm archipelago

Leif Abrahamsson, Brodd Leif Andersson

Issuing organization	Report number, ISRN	Report type
FOI – Swedish Defence Research Agency Systems Technology SE-172 90 Stockholm	FOI-R--0300--SE	Methodology report
	Research area code 4. C4ISR	
	Month year December 2001	**Project no.** E6012
	Customers code 1. Research for the Government	
	Sub area code 43 Underwater Surveillance Sensors	

Author/s (editor/s)	Project manager
Leif Abrahamsson Brodd Leif Andersson	Ilkka Karasalo
	Approved by
	Sponsoring agency Swedish Armed Forces
	Scientifically and technically responsible Ilkka Karasalo

Report title

Inversion of seabed parameters in the Stockholm archipelago

Abstract (not more than 200 words)

The purpose of this work was to apply acoustic inversion to a bay in the Stockholm archipelago with strong variations of the bottom both vertically and horizontally. The inversions were based on measurements undertaken in May 2001 of transmission loss over a 2.5 km long track. The bottom parameters were estimated by minimizing the difference between simulated and measured data. The parabolic wave equation was used as a wave propagation model and the inversions were carried out by a genetic algorithm. They resulted in a relatively good fit. The inverted bottom parameters were also evaluated by model predictions against a control data set of other frequencies than those of the inversion. The agreement between the estimated and measured parameters was good.

Keywords

Underwater acoustics, transmission loss, inversion, genetic algorithm, wave propagation model, sensitivity analysis

Further bibliographic information	**Language** English
ISSN 1650-1942	**Pages** 31 p.
	Price acc. to pricelist **Security classification**

Utgivare	Rapportnummer, ISRN	Klassificering
Totalförsvarets Forskningsinstitut - FOI	FOI-R--0300--SE	Metodrapport
Systemteknik	**Forskningsområde**	
172 90 Stockholm	4. Spaning och ledning	
	Månad, år	**Projektnummer**
	December 2001	E6012
	Verksamhetsgren	
	1. Forskning för regeringens behov	
	Delområde	
	43 Undervattenssensorer	

Författare/redaktör	Projektledare
Leif Abrahamsson	Ilkka Karasalo
Brodd Leif Andersson	**Godkänd av**
	Uppdragsgivare/kundbeteckning
	Försvarsmakten
	Tekniskt och/eller vetenskapligt ansvarig
	Ilkka Karasalo

Rapportens titel (i översättning)

Inversion av bottenparametrar i Stockholms skärgård

Sammanfattning (högst 200 ord)

Syftet med detta arbete var att tillämpa akustisk inversionsmetodik på ett område i Stockholms skärgård med stora bottenvariationer såväl vertikalt som horisontellt. Inversionerna baserades på mätningar, utförda i maj 2001, av transmissionsförluster längs en 2,5 km lång sträcka. Bottenparametrarna uppskattades genom att minimera skillnaden mellan modellberäknade och uppmätta värden. Den paraboliska vågekvationen användes som ljudvågsutbredningsmodell, och inversionerna genomfördes med en genetisk algoritm. Dessa resulterade i relativt god anpassning mot uppmätta data. De inverterade bottenparametrarna utvärderades sedan genom simuleringar och jämförelser mot kontrolldata för frekvenser som inte hade använts i inversionen. Överensstämmelsen mellan beräknade och mätta parametrar var relativt god.

Nyckelord

Undervattensakustik, transmissionsförlust, inversion, genetisk algoritm, vågutbredningsmodell, känslighetsanalys

Övriga bibliografiska uppgifter	Språk Engelska
ISSN 1650-1942	**Antal sidor:** 31 s.
Distribution enligt missiv	**Pris: Enligt prislista**
	Sekretess

Contents

1 Introduction

The purpose of acoustic inversion is to find environmental data which can be plugged into wave-propagation models for accurate prediction of acoustic wavefields in the sea. One should note that these data may not be physically relevant, they should rather be viewed as socalled equivalent media which give the same propagation features as the true media for the specific acoustical application of interest. For example: when one considers wave propagation over long ranges, the sound propagation is almost horizontal. This implies that the wave interaction with the seabed is confined to the upper part, and thus the characteristics of the seabed deeply below the seafloor is less important. In such a case a simplified equivalent seabed model which ignores the deeper structure of the seabed should be sufficient for accurate transmission loss (TL) predictions in the same frequency range for which the inversion was undertaken. Of course, it is also of interest to find out how well the bottom parameters can be determined by low-frequency transmission loss data. Needless to say, ground truth makes the model predictions more reliable with respect to seasonal variations of the water level and the sound velocity profile.

The inverse problem consists of repeatedly solving the forward wave propagation problem for different combinations of environmental parameters. A search algorithm is used for searching the optimal combination of these parameters, that is, the combination which minimizes the model-data mismatch. Since the mid-90s the Genetic Algorithm (GA) approach has been used for estimation of geoacoustic parameters at FOI. In [1] the range-independent full-field code RPRESS [2] and the range-dependent fluid PE-code FEPE [3] were used together with a GA for estimation of seabed parameters from transmission loss data recorded in the strait between the island Öland and the mainland of Sweden in 1992. That report emphasized the need for a computational model which can handle range-dependent geometries with the seabed modelled as a solid. In [4] the range-dependent fluid-solid PE-code JEPE-S [5] was applied to TL-data from one of the test-sites in [1]. As a result the model fields did adjust better to the field data, especially for the lowest frequency. In [6] the range-independent normal mode code MODELOSS [7] was incorporated in a GA for inversion of TL-data recorded over long distances in the southern Baltic. The results were encouraging except for a case where the recorded sound velocity profile had a pronounced sound channel effect. Inversion with JEPE-S and a GA [8] didn't succeed any better. A possible reason for this could be lack of information about the variability of the sound velocity profile with range.

In the inversions above the variation of the media parameters w.r.t. range was rather modest. In May 2001 a sound transmission loss experiment was carried out in a shallow bay in the southern Stockholm archipelago. The object of this experiment was to perform inversion in an environment within the belt of skerries which is both strongly range-dependent, and in reality is also far from 2D because of the vicinity to land. Impedance-estimates [9] from the same site, based on FARIM [10] (Frequency Analysis based Roughness and Impedance estimation Method) analysis of available SGU (the

Swedish Geological Survey) data, were also to be evaluated.

The inversions resulted in good fit to the measured data. The fit was almost equally good when the inverted parameters were evaluated by model predictions against a control data set for other frequencies and hydrophone depths than those of the inversion. A notable inversion result is that the velocity of the sediment drops by some 500 m/s along the track. This also demonstrates that the wave propagation model must be able to handle the fairly large geoacoustical variations by range at the current test site.

Our results are subject to a few provisions. One unsettled concern is whether the accuracy of PE-modelling is good enough in the present case. Another one is the effect of uncalibrated data on the inversion results. As a consequence only the shape of the transmission loss curves by range was accounted for in the fitness function. In future work both the experimental facilities and the wave propagation models need to be improved.

The scope of the report is the following: In Sec. 2 the experiment and the received data are described. Sec. 3 gives a brief overview of the PE-models being used in this study. Finally, in Sec. 4 the results of the seabed parameter inversions with JEPE-S and a GA are presented.

2 The Transmission Loss measurements

A sound transmission loss experiment was carried out in a shallow bay in the southern Stockholm archipelago in May 2001. The object of this experiment was to collect data for performing inversion in a complex environment within the belt of skerries, which besides being strongly range-dependent, in reality is also far from 2D because of the vicinity to land and islets. Earlier impedance-estimates [9] based on FARIM-analysis [10] of available SGU-data were also to be evaluated.

2.1 The experimental setup

The data-collection work was carried out by FOI, using the test vessel HMS Urd. A transmitter was towed at a constant depth (between 5 and 15 m) at low speed (1.5-2 m/s) along a 3 km linear track and transmitted a CW signal between 35 and 375 Hz. The transmitter, i.e. the Low Frequency Projector of the Thomson-Marconi Sonar Test System 701 (RAMSE), is a modified Gearing and Watson UW350 Hydrosounder which is a permanent magnet moving coil Acoustic Projector. Its operating frequency range is 30 Hz to 2500 Hz. There were problems with the depth-sensor why the depth of the transmitter had to be estimated. The accuracy should be within 1 or 2 m.

The signals were received by a vertical array of 8 equidistant Thomson hydrophones. The uppermost receiver was located 2 m below the water surface, the remaining following with a distance of 3.3 m between each other to the lowermost at depth 25.1 m, 2.7 m above the seabed at depth 27.8 m. The received analog signal was converted to an

optical signal which was transmitted to a PC at land via fiber. After the experiment the hydrophones were calibrated at FOI. It should be noted that the calibration was done for the frequency range 2-20 kHz, since during the experiment also sequencies of pulses (CW- and FM-pulses) with center-frequency about 7 kHz were registered. Because of limited resources within the project, the corresponding calibration of the lower frequency region which is of interest for sediment parameter estimation by wave propagation models could not be done. By this reason we have to leave out from consideration the absolute sound level of the data, hence restricting the analysis to matching of the shapes of the data. A corresponding uncertainty in the results of the inversions is thus achieved. For further discussions, see Sec. 4 below.

The sound velocity profile was measured several times and at several spots along the track during the experiment. The velocity conditions were stable w.r.t. both time and position, showing a decay in the velocity from the surface down to 20 m, and a constant velocity below that depth. The meausured sound velocity profiles are shown in Fig. 2.1 together with the profile used in the inversions.

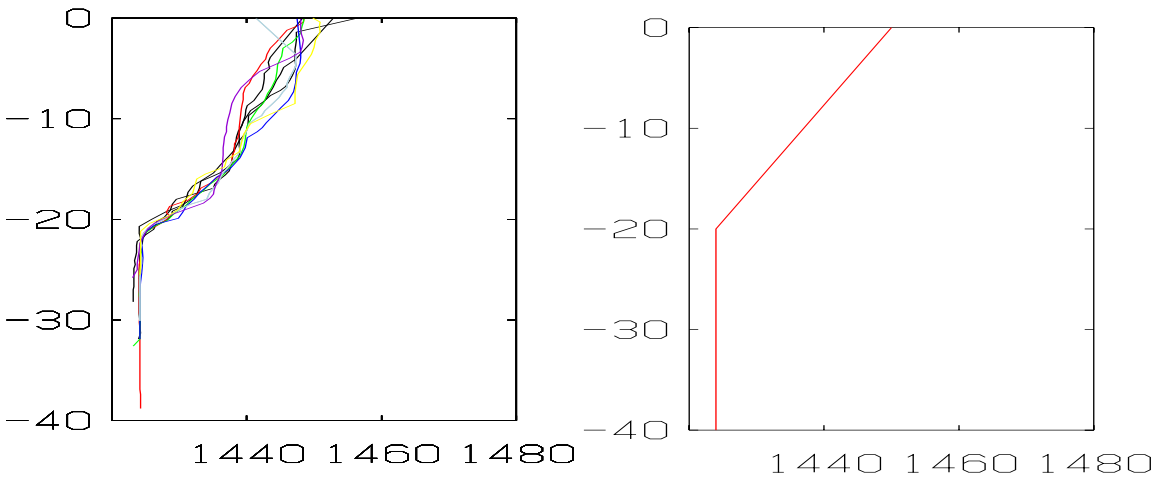

Figure 2.1: (Left) Sound velocity profiles (m/s) as function of depth (m) measured at different spots and times along the experimental track during the experiment. (Right) Sound velocity profile (m/s) as function of depth (m) used in the model inversions.

The bathymetry along the track was determined by echo sounder. The 3D-character of the bottom is striking at the shallow spot at about 1000 m, see Fig. 2.2.

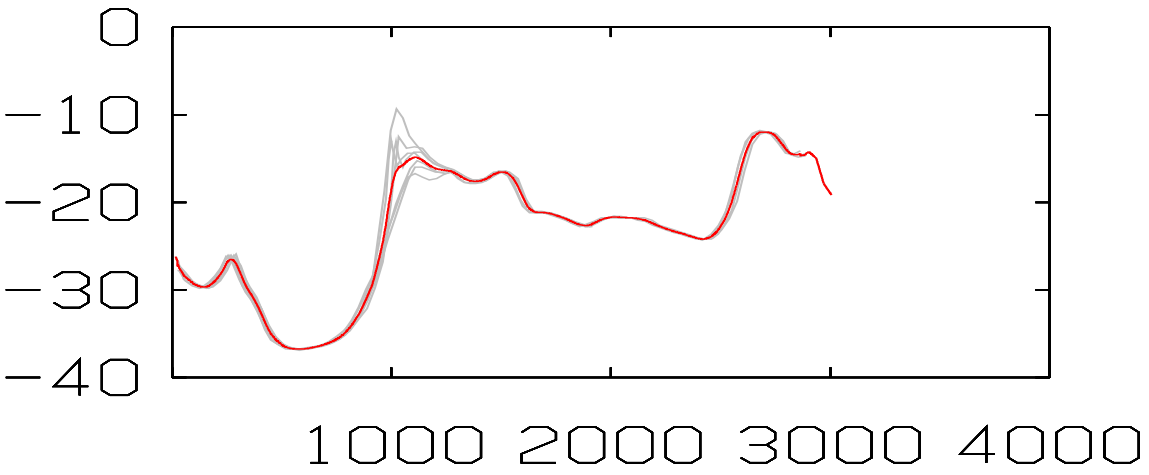

Figure 2.2: The bathymetry (depth (m) as function of range (m)) along the experimental track. The depths registered by the echo sounder are shown in grey. The average depth used in the model inversions is shown in red.

The bathymetry was registered at each of the seven CW-transmission trials. Though the test vessel essentially ran the same track all seven times, the position could differ from the expected with up to at most 10-20 m. This small difference between the tracks caused the striking difference in depth at about 1000 m (grey curves in Fig. 2.2). The reason for this is that the track ran close to land, and this shallow part of the track is an offshoot from a nearby islet. In the model inversions presented in Sec. 4 below, an average of the seven registered bathymetries is used (red curve in Fig. 2.2).

2.2 The recorded data

The measured data, which were recorded at a sampling rate of 44.1 kHz, were analyzed by FFT. At each second the power of the signal was defined as the power in a narrow band (bandwidth = 6 Hz) centered around the current frequency of interest. The frequency analysis was based on time-windows of length 2 s. A notable feature of the data is that the lower the frequency, the noisier are the data. Visual inspection of when the sharp peak at the frequency of interest in the narrow band is blurred out and hence the signal is embedded in the background noise, gives the approximate ranges from the receiver array over which the data are reliable, shown in Table 2.1.

The reason why the lower frequencies are more noisy is not clear (the receivers were not calibrated for these low frequencies). Actually, the experimental conditions were perfect when the registration of the 35 Hz signal took place late in the evening, nearly no disturbances from the surroundings were noticed.

The restricted range of reliability of the lower frequency data reduces their importance in the inversion modelling in the same sense. Hence the possibility of making good estimates of the shear parameters in the seabed decreases (see Sec. 4). Since a farfield model is used in the inversions, the comparison between the model and data must take

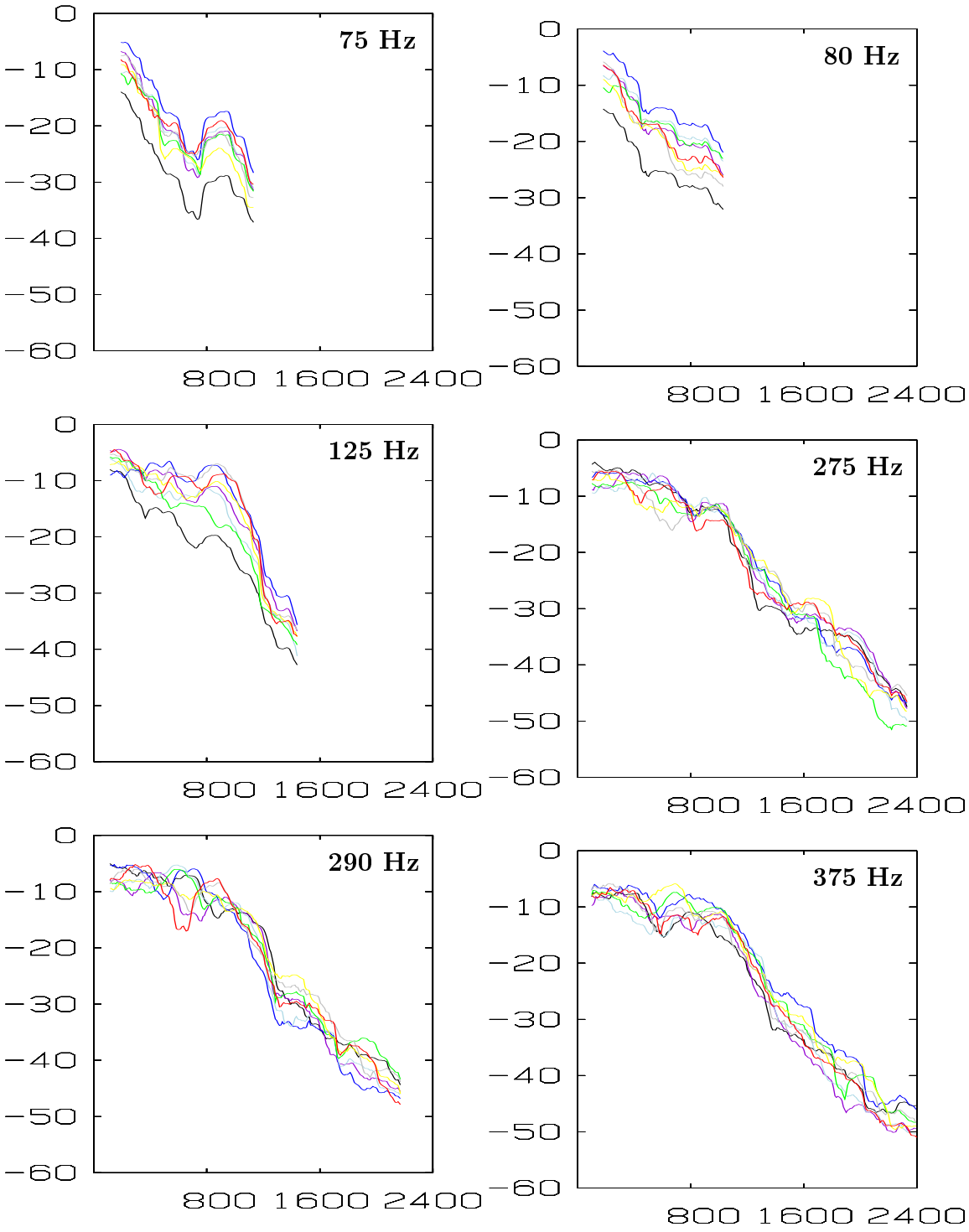

Figure 2.3: Transmission Loss data (dB) from the May 2001 experiment as function of range (m) at the 8 receivers with the following depths: 2 m = black, 5.3 m = dark violet, 8.6 m = blue, 11.9 m = light blue, 15.2 m = green, 18.5 m = yellow, 21.8 m = grey and 25.1 m = red.

Frequency	Reliable Data range
35 Hz	650 m
75 Hz	1130 m
80 Hz	1030 m
125 Hz	1440 m
275 Hz	2330 m
290 Hz	2170 m
375 Hz	2400 m

Table 2.1: Ranges from the receiver array over which the recorded data are reliable.

place not closer than at a certain minimum distance from the source. As a rule of thumb this distance should be about 10 wavelengths. The wavelength in water at frequency 35 Hz is about 40 m, and hence the 35 Hz data are useless for our analysis.

The transmission loss of the remaining six frequencies in the reliable range intervals, after smoothing of the power by a sliding rectangular window of length 200 m, are shown in Fig. 2.3. The corresponding transmitter-depths for these frequencies are shown in Table 2.2.

Frequency	Source Depth
75 Hz	5 m
80 Hz	8 m
125 Hz	8.5 m
275 Hz	14.5 m
290 Hz	8 m
375 Hz	8 m

Table 2.2: Transmitter-depths.

3 Forward modelling codes

In this study the parabolic wave equation (PE) has been used as a model of acoustic and elastic wave propagation in a range-dependent environment. PE is an approximation to the full wave equation, or the Helmholtz equation (HZ) in the time-harmonic case. The validity of PE-modelling is limited to one-way propagation within an angular cone $\lesssim 40^o$ with respect to the horizontal axis. Within this angular domain all wave features like reflection, refraction, diffraction etc. are accurately reproduced. PE is a far-field approximation and its modelling ability improves at higher frequencies. The use of PE at low frequencies in shallow waters with large changes in bathymetry is more problematic [11].

For a long time there has been a continual development of PE codes at FOI [12, 13, 5]. The software, named JEPE, (Jetsch Energy conserving PE) is rather a toolbox of modules for data processing, acoustic sources, step integrators etc, than a single program. In this study we have used two versions, JEPE-S and JEPE-I, with somewhat different capabilities.

3.1 JEPE-S

JEPE-S is a propagation code for range-dependent layered fluid-solid media. The theoretical model and the numerics of JEPE-S are well documented [5, 14]. It has served as the main forward model in previous inversion studies [4, 8].

3.2 JEPE-I

JEPE-I is aimed at being an extended aid in solving inverse problems. Besides providing forward PE-modelling, it offers inversion algorithms and tools for sensitivity analysis. Work on JEPE-I started recently and it is still incomplete. Therefore only part of its potential was exploited in the current application. A brief account of some key features follows below.

3.2.1 Computation of derivatives

The derivatives of the wave field or the objective function with respect to target parameters are of special significance in inverse theory and optimal control [15, 16]. For example, they make up the Jacobian matrix of the linearized least-squares problem [8]. The columns and rows of the pseudo-inverse of the Jacobian display the influence of each data point and the sensitivity of the model parameters. The condition number of the Jacobian reveals redundancies or linear dependencies among the inversion parameters. Information on the Hessian of the object function can be extracted by discrete approximations based on the gradient. Besides being a tool for data and model analysis, the availability of the Jacobian enables optimization methods based on the Gauss-Newton approach [17, 18]. The derivatives satisfy the same discrete PE-model as the solution itself except for zero initial conditions and a forcing term involving the derivative of the target parameter and the PE-solution. Therefore all wanted derivatives can be computed simultaneously by a single call to a PE-solver with a multiple right hand side. Yet there is a less expensive alternative if merely the gradient of the object function is needed. This approach exploits duality and requires only one solution of the adjoint PE equation in which point sources are placed at the positions of the observation points. Optimization methods of quasi-Newton type rely on the computation of the gradient.

3.2.2 Multiple sources and reciprocity

Like the present study, a common experimental setup is to use a stationary array of hydrophones while the source is towed at a low speed. However, from a computational point of view it is more convenient with a fixed source. This can be achieved by an exchange of source and receiver locations due to the reciprocity principle. In doing this we arrive at a PE-model with sources at the depths of the hydrophones. The corresponding solutions can be computed simultaneously as they satisfy the same PE-model. This is just another case with the same equation with a multiple right hand side. Taking this into account is a cost effective measure as compared to separate runs for each source.

3.2.3 Bottom roughness and volume scattering

Occasionally the inverted absorption coefficient of the seabed turns out to be quite large (1-2 dB/λ) [6, 8]. One plausible explanation is the absence of surface roughness in existing low-frequency transmission loss codes. To test this hypothesis there is an option of JEPE-I to modulate a smooth interface by stochastic perturbations. The probability density distributions of the size and shape of surface roughness is governed by input parameters which are passed to pseudo-random number generators. However, there is no statistical treatment of the PE-model itself and an ensemble average must be formed by running a large number of realizations. To be consistent with angular constraint of the PE-model there should be a predominance of scattering in the forward direction. It implies that the surface roughness must meet the Rayleigh criterion [19]. In the same fashion, it is possible to introduce randomized volume scatterers of different types and amounts. It should be remembered though, that the geometric setting is 2D.

3.2.4 PE-modelling in rough geometries

For computational purposes the sea-seabed environment is usually grouped into layers. Acoustic media parameters are ascribed to each layer. They may vary by both range and depth. In JEPE-I the layered structure is relaxed in the sense that layer boundaries may intersect each other. In addition, enclosures may be superimposed on a layered background. An enclosure is usually specified as one or several closed polygon chains. The PE-solution is computed on a uniform Cartesian grid, and acoustic data at grid points are picked from the overlaying geometric element (layer/enclosure/stochastic perturbation) with the highest priority (user assigned). The prescribed hierarchy of the mosaic of overlapping geometric elements dispenses with the cumbersome task of finding their intersection points.

3.2.5 Transparent boundary conditions

The computational domain of a PE-model must be finite in depth, and the convential approach is simply to truncate the bottom at a large depth. To prevent backreflections from a false boundary deep down, artifical absorption is added in an increasing amount by depth. An alternative is to employ transparent boundary conditions which simulate the acoustic response of an infinite, homogeneous bottom [20]. This technique was recently evaluated in [21] and adopted in JEPE-I. As a result, in the current application the computational domain could be confined within a depth of 100 m for all frequencies.

3.2.6 Checking the validity of the PE-model

At low frequencies and large environmental changes by range the accuracy of the PE-model becomes a serious concern. The fidelity of PE-modelling is hard to assess in advance since it depends on the seabed parameters, the frequency and the angular width of the source and receiver positions. However, it is possible to contrive 'sensors' which monitor the foundation of the PE-model as the wave field evolves. An inexpensive measure is to check the energy balance

$$
\begin{aligned}
P_{source} = \quad & P_{diss} + P_{out}, \\
\\
P_{source} = \quad & \text{power of source} \\
P_{diss} = \quad & \text{dissipated power due to absorption} \\
P_{out} = \quad & \text{power flux out of the computational box}
\end{aligned}
\tag{3.1}
$$

All terms in the conservation law (3.1) are easily evaluated as surface and line integrals once the solution is known. They are updated incrementally as the solution is advanced in range. In the end, the performance of the PE-model is condensed into a Figure of Fidelity (FoF) defined by

$$
\text{FoF} = 100 \max_{range} |1 - |\frac{P_{source} - P_{diss} - P_{out}}{P_{source}}|| \tag{3.2}
$$

that is, FoF expresses in percent how well the energy balance is met. Comparisons with full-field models [7, 11], indicate that FoF is not equivalent to an error estimate of transmission loss in dB. By experience, FoF seems to be a too sensitive measure in that respect.

4 Results of seabed parameter inversions

In situ measurements in the 1.5 m thick gyttja clay layer close to our test site have indicated a mean velocity in the sediment of about 1450 m/s. Laboratory analysis of core samples shows a bulk density just above 1500 kg/m^3. The corresponding impedance is 2.2 $\times 10^6$ $kg/m^2 s$, a value that can be expected for the type of material in this area. On the other hand, analyses of echoes from bottom penetrating parametric sonar by the FARIM-method [10] have indicated values of the acoustic impedance close to 1.6 $\times 10^6$ $kg/m^2 s$ [22]. A possible explanation for this discrepancy could be the presence of "micro" bubbles of gas in the sediment [23].

The track of the test vessel in our experiment in May 2001 crossed a fracture zone, located at the deep part of the bathymetry between 300 and 900 m in Fig. 2.2, with migrating thermogenic gas contained in the sediment. Within this area one should therefore expect larger quantities of gas than at the closely located test site mentioned above. Bottom penetrating sonar and reflection seismics data collected by SGU indicates a 5-10 m thick gaspocket between 400 and 800 m. Taking these geological considerations into account, a reasonable estimation of the acoustic parameters in this pocket would be a bulk density of about 800 kg/m^3 and a sound velocity of about 800 m/s, thus giving an acoustic impedance of 0.64 $\times 10^6$ $kg/m^2 s$ [23]. However, FARIM-analysis of the data gives the same value of the impedance as at the nearby site above [9]. This could be due to a similar gyttja clay layer on top of the gas-reservoir, which acts as a reflector for the high frequencies used in that analysis (dominating frequencies about 7 kHz).

An object of our experiment was to evaluate this result by our range-dependent wave propagation models applied to low-frequency transmission loss data. However, simplifications had to be done in the geometrical configuration of the inversion models so

that JEPE-S succeeded to transform each layer of the geometry to a rectangle in the transformed space. By this reason we were not able to introduce a gaspocket with distinct vertical boundaries at 400 and 800 m respectively in the inversions. Furthermore, the layer thicknesses are not allowed to shrink to zero anywhere, why the outcrop of the bedrock at the shallow part of the track at about 1000 m, could not be modelled by JEPE-S in the GA-inversions. These limitations of the model are in some degree compensated for by the possibility of allowing the media parameters to vary smoothly w.r.t. both range and depth within each layer. As a consequence we tried to adjust a simple 3-layer model, consisting of a water-layer, one sediment and a bedrock, to the TL-data by letting the geoacoustic parameters of the sediment vary as functions of both range and depth.

The TL-data were measured at an array which was fixed in space while the source was moving. However, the computational model requires a fixed source. Due to the reciprocity principle of linear acoustics the positions of the source and receivers can be interchanged. Because of the range-dependent configuration this can be done for only one source depth and one receiver depth at a time. Thus the cost for comparing the data and model fields is proportional to the product of the number of frequencies and the number of receiver depths. There is therefore a need for restricting the number of receivers which are to be used in the inversion. Since the gradient of the sound velocity profile in the water was negative (Fig. 2.1), we had reasons to believe that we should do well with using only the lowermost receiver in the array (depth=25.1 m) in the inversions. Furthermore, the data curves for each of the six frequencies recorded by the eight receivers show no essential differences between each other as functions of receiver depth (Fig. 2.3). From these six frequencies we chose four to be used in the inversions, namely 75, 125, 275 and 375 Hz. As control data we used all six frequencies at the remaining seven receiver depths.

The objective function, which gives a measure of the model-data mismatch, is defined as the mean l_2-norm of the difference between the model and data dB-values for all frequencies and receiver depths and ranges. Because of lack of calibrated data, the model-curves for each frequency have been adjusted by a constant in order to minimize the objective function. This means that we are only trying to adapt the shapes of the model fields to the field data.

Three GA-inversions with JEPE-S were done, two with a fluid seabed model and one with a solid seabed. In the water we used the sound velocity profile in Fig. 2.1. The bathymetry of Fig. 2.2 (red curve) was also used. The conditions of the bedrock were assumed to be known: density = 2650 kg/m^3, sound velocity = 5500 m/s and attenuation = 0.2 dB/λ. In the solid case we added the shear velocity = 2700 m/s and the shear attenuation = 0.1 dB/λ. The same GA as in [4, 8] was used. In each of the three inversions 6 populations were used with 1000 individuals in each and 500 model evaluations/population before migration took place, at which the 4 best individuals of each population were migrated to the other populations. 4 migrations took place, which amounts to a total of 21000 fitness-evaluations, or 84000 runs of JEPE-S since

4 frequencies were matched. The runtime on a PC-cluster consisting of 17 nodes was about three days. The wide-angle JEPE-S with a source field containing propagating modes with propagation angles 30 degrees or less was used for the model evaluations. The fields were computed on the same range grids as the original data (stepsize about 1.5 m) and smoothed with the same sliding rectangular window of length 200 m as was used for the smoothing of the data. The smoothed data and model-values were matched on range grids with stepsize 10 m. The results of the inversions are presented below.

4.1 Fluid media inversion 1

Inversion was made for all three acoustic parameters in the sediment. The density and attenuation varied as functions of range only, the sound velocity could vary with depth as well. The thickness of the sediment was also incorporated in the inversion scheme. All media parameters were sought for at five range points: 117, 267, 617, 1117 and 1517 m respectively. Outside this range the parameters were constantly extrapolated. JEPE-S represents the media parameters by splines of degree 5. Except for the thickness-parameter, which was allowed to vary in the interval 10-40 m at the last range point, the search intervals for all parameters were the same at all range points. The search intervals are found in Tab. 4.1 (v_p^{top} denotes the velocity at the water/sediment-interface, $\partial v_p/\partial z$ the gradient of the velocity w.r.t. depth).

Parameter	Search interval	Number of bits
ρ [kg/m^3]	(800, 2000)	4
v_p^{top} [m/s]	(1100, 1800)	6
$\partial v_p/\partial z$ [1/s]	(0, 25)	4
β_p [dB/λ]	(0.1, 2.0)	4
thickness [m]	(10, 30)	5

Table 4.1: The parameter intervals where the GA sought the optimal environmental model using JEPE-S.

There were thus in all 25 parameters (represented by 115 bits, which amounts to $2^{115} = 4.2 \times 10^{34}$ points in the search space) to be optimized by the GA. The media parameters obtained from the inversion are shown in Fig. 4.1. The fitness values for the inversion data set (4 frequencies and one receiver depth (hydrophone 8)) and the control data set (6 frequencies and 7 receiver depths (hydrophones 1-7)) are shown in Tables 4.2 and 4.3 respectively.

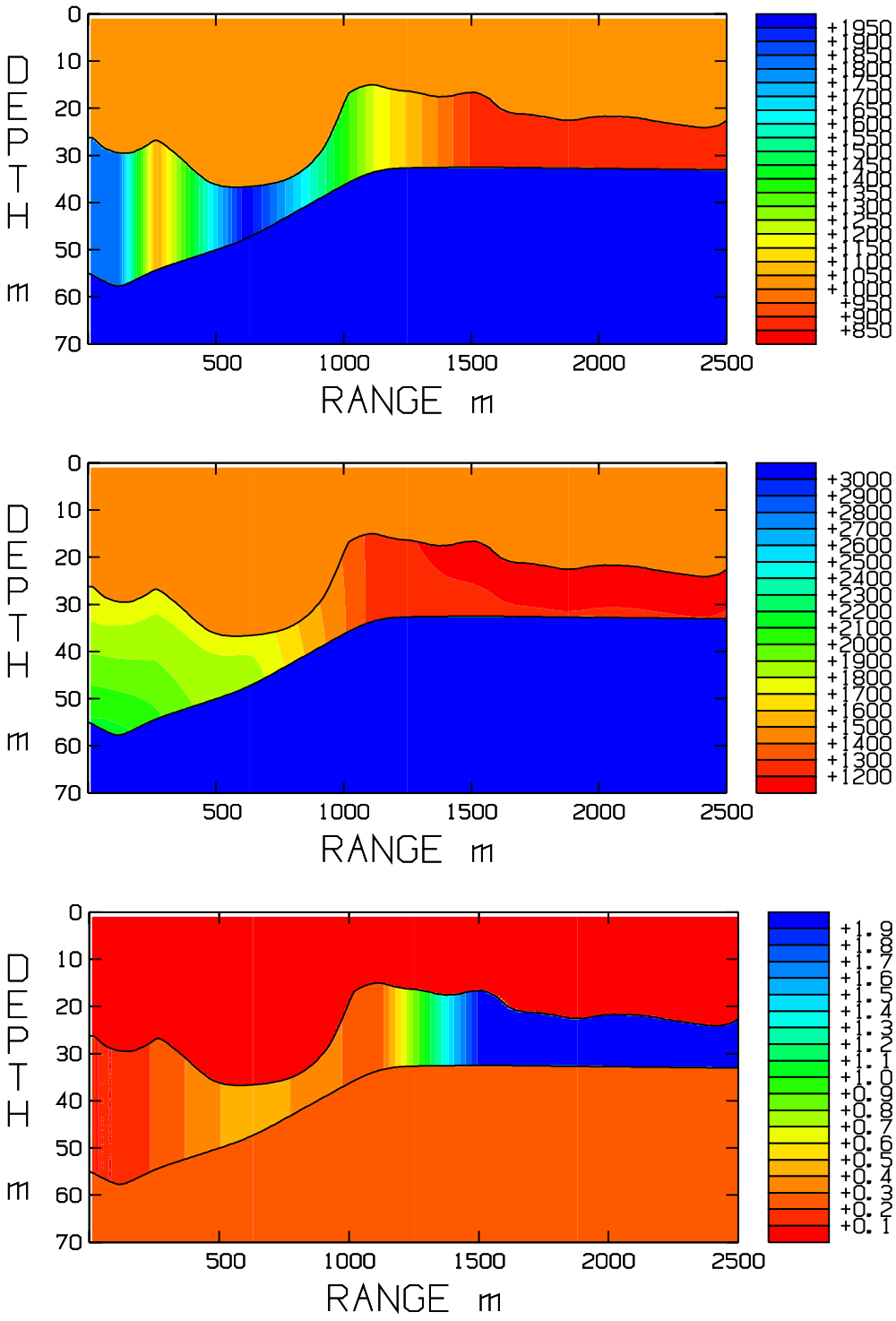

Figure 4.1: Media parameters obtained from fluid media inversion 1: density [kg/m^3] (top), p-velocity [m/s] (middle) and p-attenuation [dB/λ] (bottom).

Frequency	Fitness
75 Hz	1.96
125 Hz	2.64
275 Hz	2.08
375 Hz	2.58
75, 125, 275, 375 Hz	2.36

Table 4.2: Fitness values for the **inversion data set** (4 frequencies, hydrophone 8) in the fluid media inversion 1.

Frequency	Fitness
75 Hz	4.85
80 Hz	4.76
125 Hz	2.84
275 Hz	4.19
290 Hz	6.36
375 Hz	3.45
All 6 frequencies	4.56

Table 4.3: Fitness values for the **control data set** (6 frequencies, hydrophones 1-7) in the fluid media inversion 1.

The results are encouraging. We notice the tremendous agreement between model and data for the inversion data set (Table 4.2). The model- and data-curves are shown in Fig. 4.2.

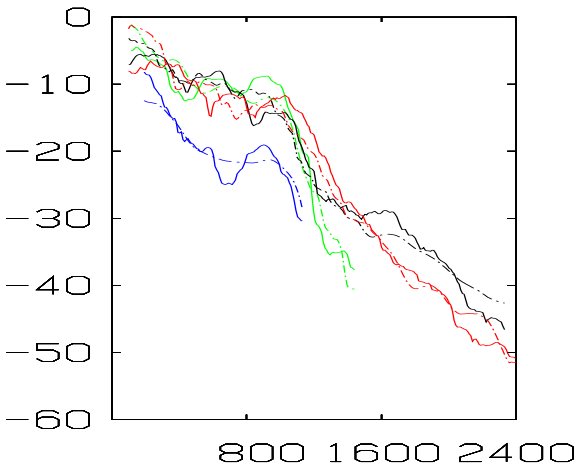

Figure 4.2: Model solution [dB] (dashed lines) and data [dB] (solid lines) as function of range [m] from fluid media inversion 1: 75 Hz (blue), 125 Hz (green), 275 Hz (black) and 375 Hz (red).

The results for the control data set (Table 4.3) are not too bad either, especially not for the frequencies 125 Hz and 375 Hz. However, the fitness value for 75 Hz is deteriorated. This can depend on the model itself, but could equally well be an effect of bad data due to differences in the sensitivity of the receivers in the array (we remind the reader that no calibration has been done for frequencies below 2 kHz). If we instead of minimizing the objective function by adjusting the whole data set for each frequency by a constant (Table 4.3), adjust the data from each receiver and frequency by a constant, then we eliminate the risk for differences in the relative sound level from the different receivers. The corresponding control data result is found in Table 4.4.

Frequency	Fitness
75 Hz	2.89
80 Hz	2.36
125 Hz	2.71
275 Hz	3.76
290 Hz	4.63
375 Hz	3.21
All 6 frequencies	3.54

Table 4.4: Fitness values for the **control data set** (6 frequencies, hydrophones 1-7) in the fluid media inversion 1 when data from each receiver are matched separately for each frequency.

We see that the fitness-values for all frequencies were improved considerably except for the frequencies 125 Hz and 375 Hz which were already well matched in Table 4.3. A possible reason for this could be that the sensitivity between the receivers did not differ for 125 Hz and 375 Hz, while it did differ for the remaining frequencies. In Fig. 4.3 the result of the calibration of the array in the frequency interval 2-20 kHz is shown. We see that in general the sensitivity of the receivers can differ between each other up to 5 dB, and that there are local variations in the frequency domain. One cannot extrapolate the behaviour of the receivers safely to the low-frequency domain, but a reasonable guess is that it is unlikely that all eight receivers are equally sensitive. Fig. 4.3 therefore emphasizes the need for low-frequency calibration of the receivers for inverse modelling purposes, otherwise one cannot make use of data from several receivers simultaneously.

A notable fact from the level plots of Fig. 4.1 is, that in spite of the supposed presence of a gaspocket with low impedance between 500 and 800 m, the inversion gives a hard sediment with impedance well above 3 $\times 10^6$ kg/m^2s. This could be due to the fact that we only match the shapes of the data curves and neglect the absolute level. To try this hypothesis we exchanged the hard bottom between 500 and 800 m in Fig. 4.1 to a soft and gassy bottom and computed the corresponding fitness-values. The medium is shown in Fig. 4.4 and the fitness-values are found in Table 4.5.

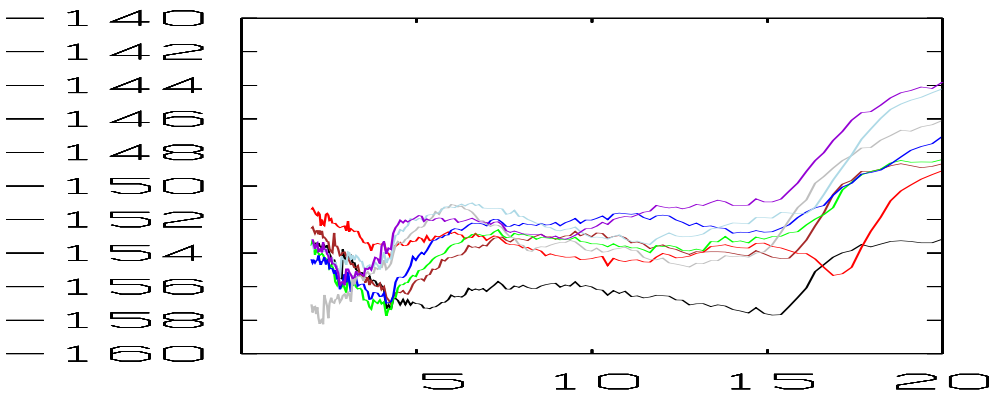

Figure 4.3: Calibration data for the receiver-array. Registered sound level [dB] as function of frequency [kHz]. Hydrophone 1 (black), 2 (brown), 3 (red), 4 (green), 5 (blue), 6 (grey), 7 (light blue) and 8 (dark violet).

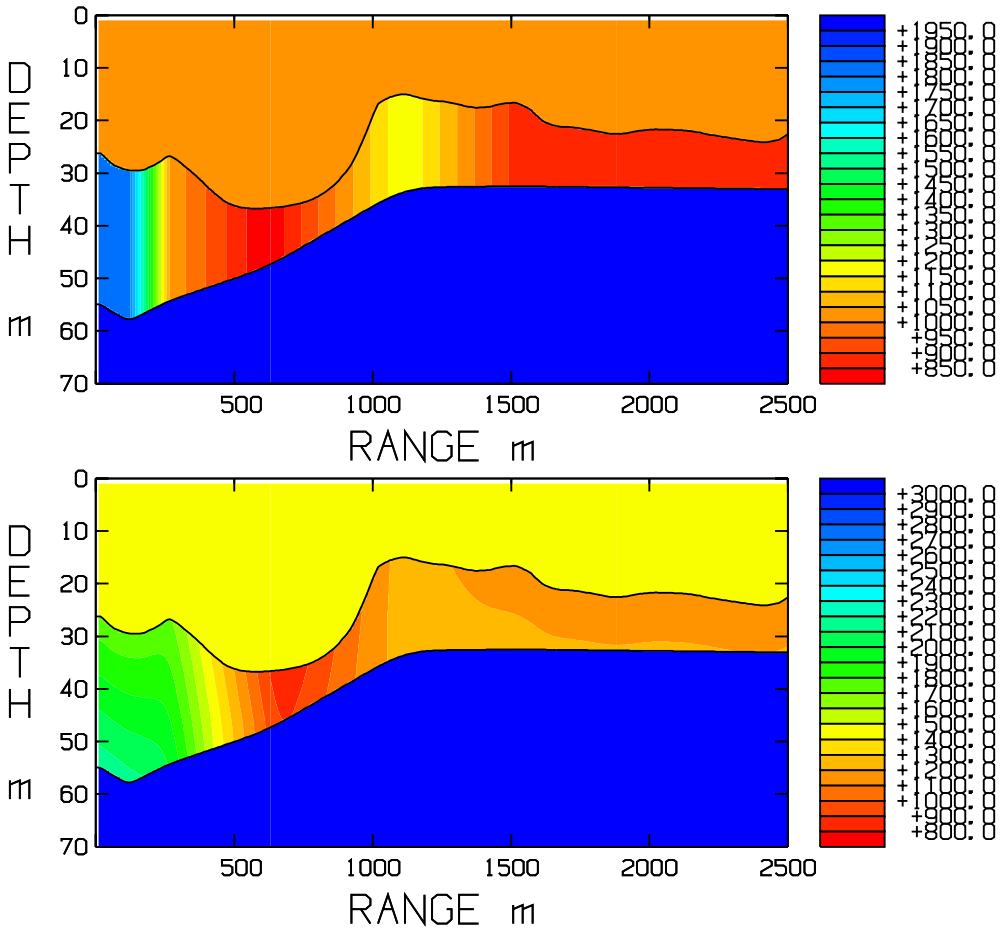

Figure 4.4: Modified media parameters from fluid media inversion 1. The hard bottom between 500 m and 800 m has been changed to a soft and gassy bottom. Density [kg/m^3] (top), p-velocity [m/s] (bottom). Observe that the scale in the levelplot of the p-velocity differs slightly from the one used in Fig. 4.1.

Frequency	Fitness
75 Hz	3.03
125 Hz	6.13
275 Hz	2.56
375 Hz	4.57
75, 125, 275, 375 Hz	4.22

Table 4.5: Fitness values for the **inversion data set** (4 frequencies, hydrophone 8) for the modified medium shown in Fig. 4.4 (cf. Table 4.2).

The deteriorated fitness-values should not be surprising since we have made a dramatic change in 2 of the 25 parameters without making any compensations in the remaining 23. The corresponding model solutions and data are shown in Fig. 4.5.

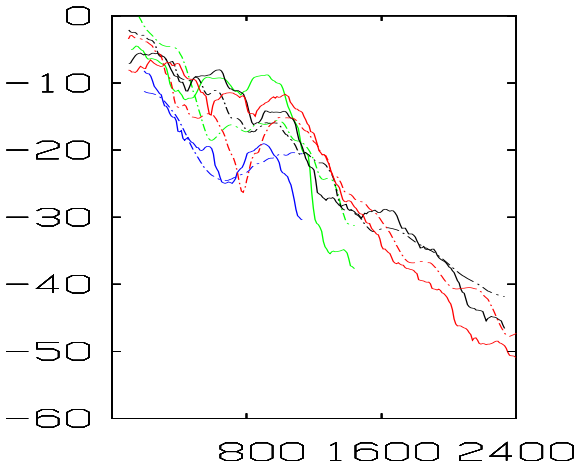

Figure 4.5: Model solution [dB] (dashed lines) and data [dB] (solid lines) as function of range [m] for the modified medium shown in Fig. 4.4: 75 Hz (blue), 125 Hz (green), 275 Hz (black) and 375 Hz (red) (cf. Fig. 4.2).

Though the fitness-value for the 75 Hz-data has increased from 1.96 (Table 4.2) to 3.03, a comparison between the model solutions in Fig. 4.2 and 4.5 respectively, reveals that the 75 Hz-solution with the worse fitness-value actually adapts better to the rate of decay of data in the first half of the range-interval than the model-solution with the better fitness-value does. In this case therefore, a model-data mismatch based on absolute sound levels should probably have favored the modified gassy layer if only the 75 Hz-data had been considered. However, the deep local minimum in the 375 Hz-solution in Fig. 4.5 (red curve) has no counterpart in the 375 Hz-data. On the other hand, a corresponding local minimum is present in the 290 Hz-data in Fig. 2.3, why the behaviour of the 375 Hz-solution is not too unrealistic.

The conclusion that can be drawn from the considerations above is that mutually well-calibrated receivers are of fundamental importance for reasonable estimation of seabed parameters by inverse modelling. But receivers which are calibrated relative to

each other is not enough, also the absolute sound level of both the transmitter and the receivers should be calibrated for the specific frequencies that are used in the inversions. Information is otherwise lost when only the shapes of the data curves are considered in the matching. These points of view should be kept in mind when we present the remaining inversion results below.

4.2 Fluid media inversion 2

In this inversion we allowed the sound velocity to vary with depth as above, but not with range. The remaining parameters and search intervals were identical with the former inversion. 17 parameters (represented by 75 bits, which amounts to 3.8 $\times 10^{22}$ points in the search space) was to be optimized by the GA. The media parameters obtained from the inversion are shown in Fig. 4.6. The fitness values for the inversion data set (4 frequencies and one receiver depth (hydrophone 8)) and the control data set (6 frequencies and 7 receiver depths (hydrophones 1-7)) are shown in Tables 4.6 and 4.7 respectively. Since we have assumed equally sensitive receivers for the control data set in Table 4.7, while it is most unlikely that this assumption is valid (cf. Fig. 4.3), the interpretation of the result is difficult. We have no other alternative than to match the data for each receiver and frequency separately as is done in Table 4.8. Compared to Table 4.4 the result has deteriorated with between 1 and 2 dB for the frequencies 75, 125 and 375 Hz, while for 80, 275 and 290 Hz the results are similar. The deterioration could depend on the fact that the sound velocity does not vary with range as in the former inversion. As is seen in Fig. 4.6, the sound velocity adopts a value close to 1450 m/s at the interface between the water and the sediment, the same value as in situ measurements have indicated as a mean velocity in the gyttja clay layer close to our test site.

Frequency	Fitness
75 Hz	3.69
125 Hz	2.63
275 Hz	2.70
375 Hz	2.81
75, 125, 275, 375 Hz	2.88

Table 4.6: Fitness values for the **inversion data set** (4 frequencies, hydrophone 8) in the fluid media inversion 2.

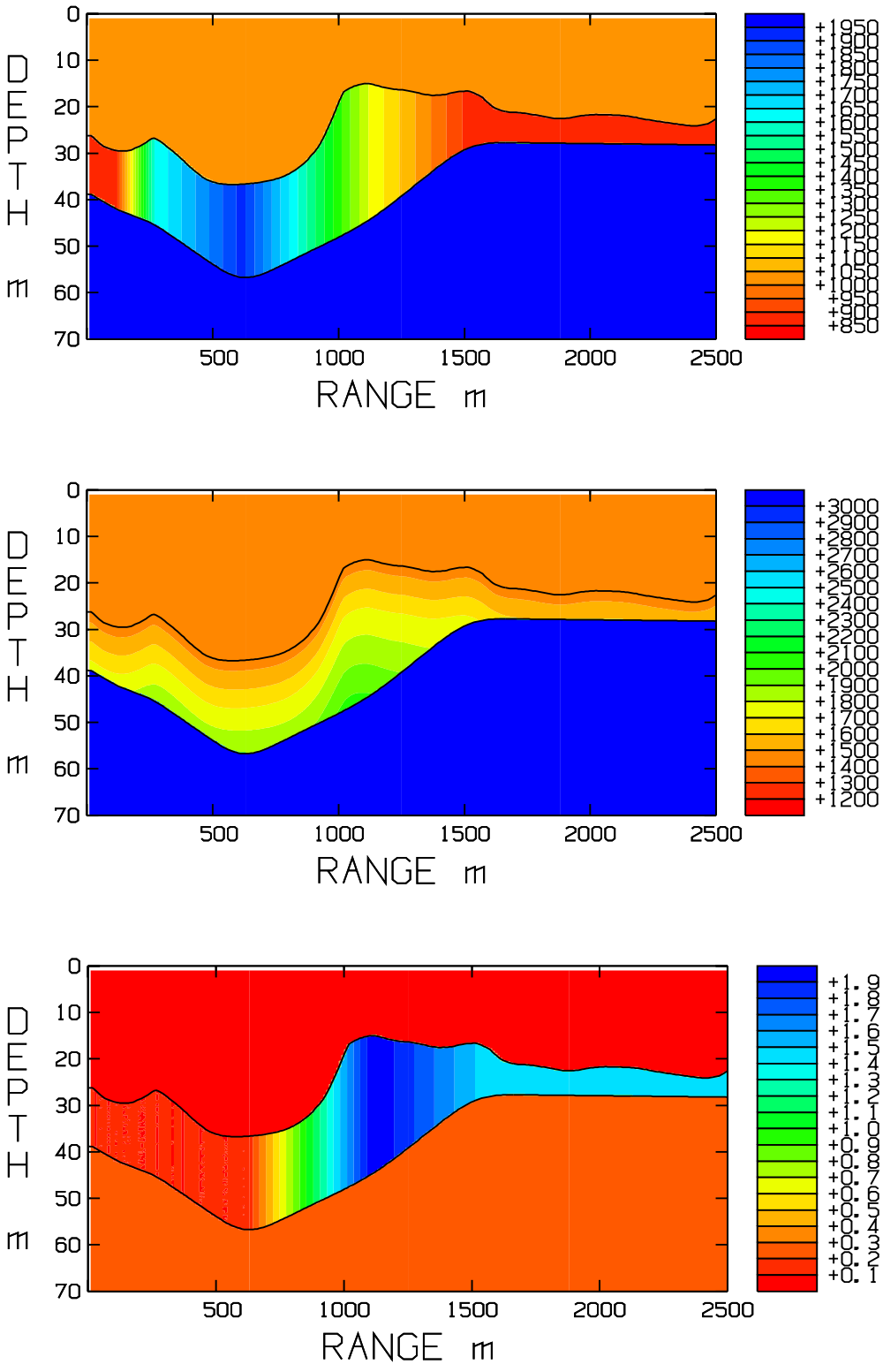

Figure 4.6: Media parameters obtained from fluid media inversion 2: density [kg/m^3] (top), p-velocity [m/s] (middle) and p-attenuation [dB/λ] (bottom).

Frequency	Fitness
75 Hz	6.00
80 Hz	3.35
125 Hz	5.15
275 Hz	5.25
290 Hz	5.51
375 Hz	5.26
All 6 frequencies	5.23

Table 4.7: Fitness values for the **control data set** (6 frequencies, hydrophones 1-7) in the fluid media inversion 2 when data from all receivers are matched simultaneously at each frequency.

Frequency	Fitness
75 Hz	4.54
80 Hz	3.00
125 Hz	4.93
275 Hz	3.54
290 Hz	4.31
375 Hz	4.41
All 6 frequencies	4.19

Table 4.8: Fitness values for the **control data set** (6 frequencies, hydrophones 1-7) in the fluid media inversion 2 when data from each receiver are matched separately for each frequency.

4.3 Model accuracy and sensitivity analysis

4.3.1 The accuracy of PE-modelling

The area between 500 and 1100 m is most troublesome as concerns PE-modelling. The water depth varies between 15 and 37 m, and the velocity of the sediment drops by some 500 m/s over this patch according to the above inversion. Prior to and beyond this transition zone the environment is only weakly range-dependent. Here a PE-model is expected to work well. However, the fairly strong range-dependence in the midarea raises concerns about the accuracy of PE-modelling. To probe this question we have applied JEPE-I to two conceivable seabed models, hereafter referred to as model A and B. Color maps of their velocity distributions are shown in Fig. 4.7.

Model A consists of three layers in which the sediment parameters were found by a genetic fit. Model B resembles the seabed structure that was synthesized by data from bottom penetrating sonar. It departs from model A by the presence of a gassy pocket (red) between 500 and 800 m. Furthermore, the bedrock protrudes the sediment, and the peak interfaces the water around 1000 m. The source depth of the simulations was set to 25.1 m (the deepest receiver depth of the actual experiment). Table 4.9 shows how well the PE-solution maintains energy conservation according to the measure (3.2).

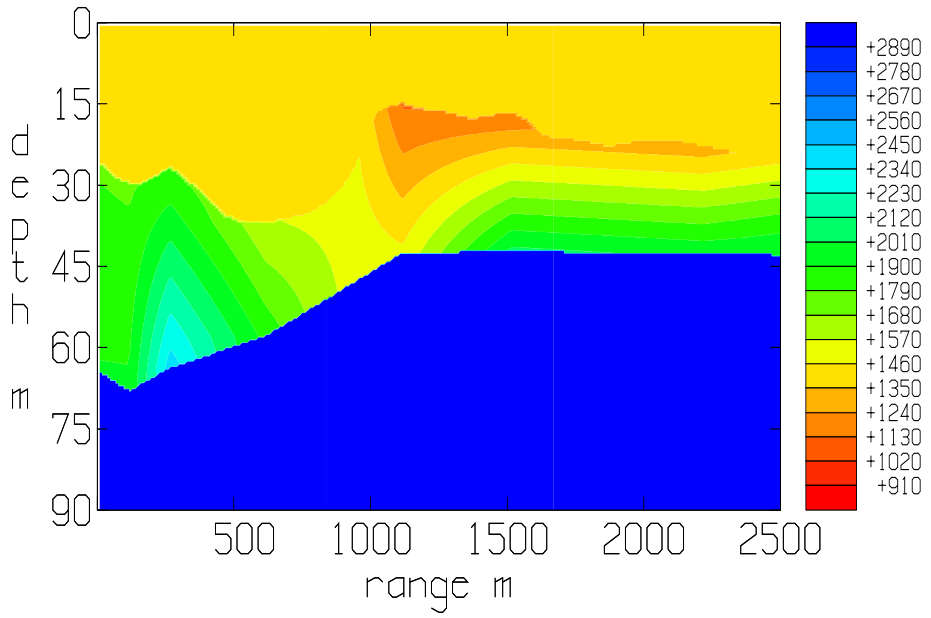

(a) model A

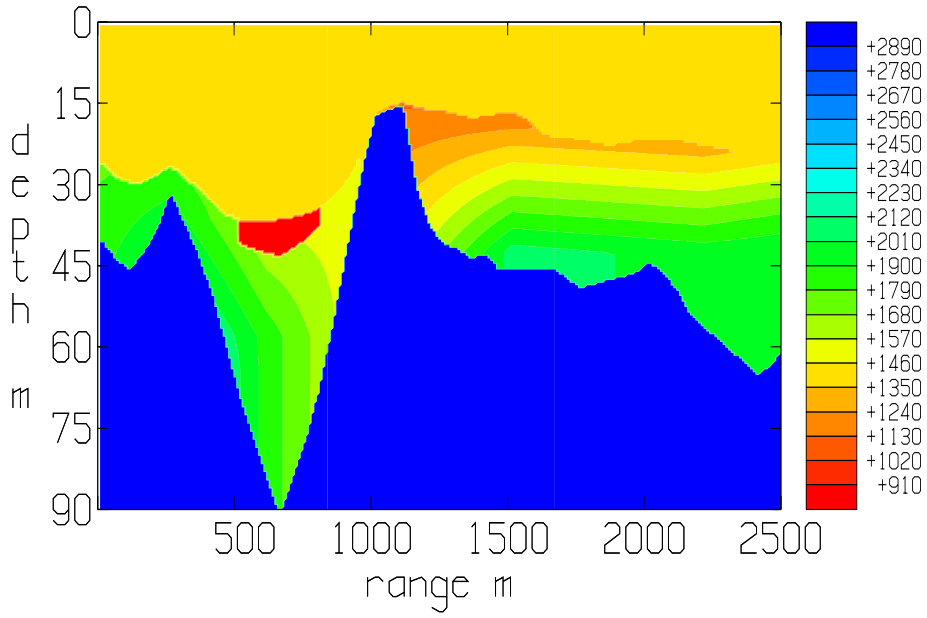

(b) model B

Figure 4.7: Color maps of the velocity distributions of two seabed models.

As can be seen, the energy balance improves by frequency despite an extended recording range. We also see a distinction between the models, in particular at the low frequencies 75 and 125 Hz. As expected, PE-modelling for model B is harder because of the stronger range-dependence. Fig. 4.8 is a plot of FoF as a function of range for 75 Hz.

frequency $[Hz]$	FoF (model A)	FoF (model B)	range $[m]$
75	89	56	1130
125	94	66	1440
275	92	75	2320
375	94	84	2400

Table 4.9: FoF (Figure of Fidelity), expressed in percent, as function of frequency. The last column is the measuring range of FoF.

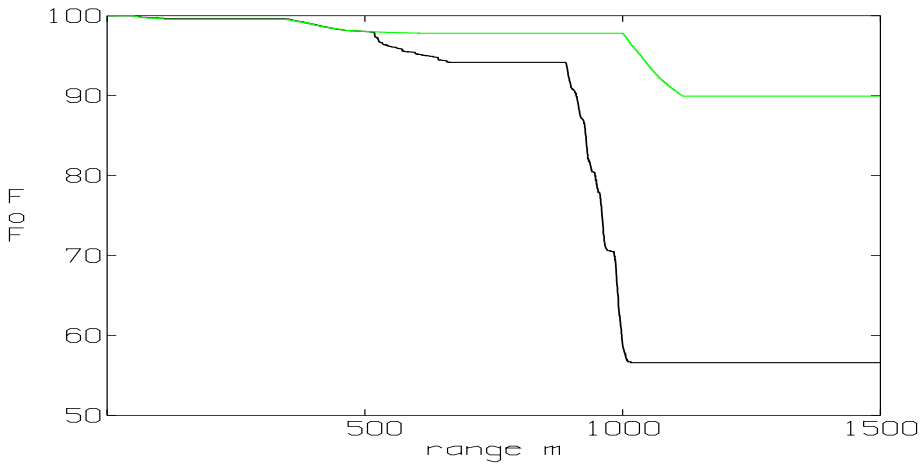

Figure 4.8: FoF for 75 Hz for model A (green) and B (black).

A comparison with Fig. 4.7 reveals that variations in range adversely affect the fidelity of the PE-model. To be able to quantify the degree of uncertainty in terms of dB, it would be necessary to invoke a Helmholtz solver.

4.3.2 Simplified inversion on a limited area

Fig. 4.8 indicates that there is a sudden drop of the accuracy of the PE-model beyond 900 m for the more complex bottom structure of model B. Therefore the inversion on this model was confined to 900 m in range. The inversion was done on data for 75, 125, 275 and 375 Hz and for two hydrophone depths (11.9 and 25.1 m). The velocity, density and absorption of the sediment were assumed to be only range-dependent with a linear variation between the range points 0, 217, 517, 717 and 917 m. In additon to these 15 parameters, those of the gaspocket were also included in the inversion. On this problem we tried the simplex method [24]. By starting the initial simplex from the above genetic fit, a local refinement could be achieved with some hundred evaluations of the fitness function. The inversion result is presented in Table 4.10, and a level plot of the velocity is shown in Fig. 4.9.

The optimal fitness value of this inversion was 2.3 dB. The evaluation on the the remaining data set (6 hydrophones and 6 frequencies) was 2.7 dB. This inversion result is similar to the one in Sec. 4.1 in the common zone up to 500 m.

range $[m]$	velocity $[m/s]$	density $[kg/m^3]$	absorption $[dB/\lambda]$
0	1525	1741	0.08
217	2313	1653	0.06
517	1822	1645	0.08
717	1497	1517	0.19
917	1738	1535	0.11
gaspocket	805	743	0.16

Table 4.10: Optimal inverted parameters of the sediment at the beginning of the test-site.

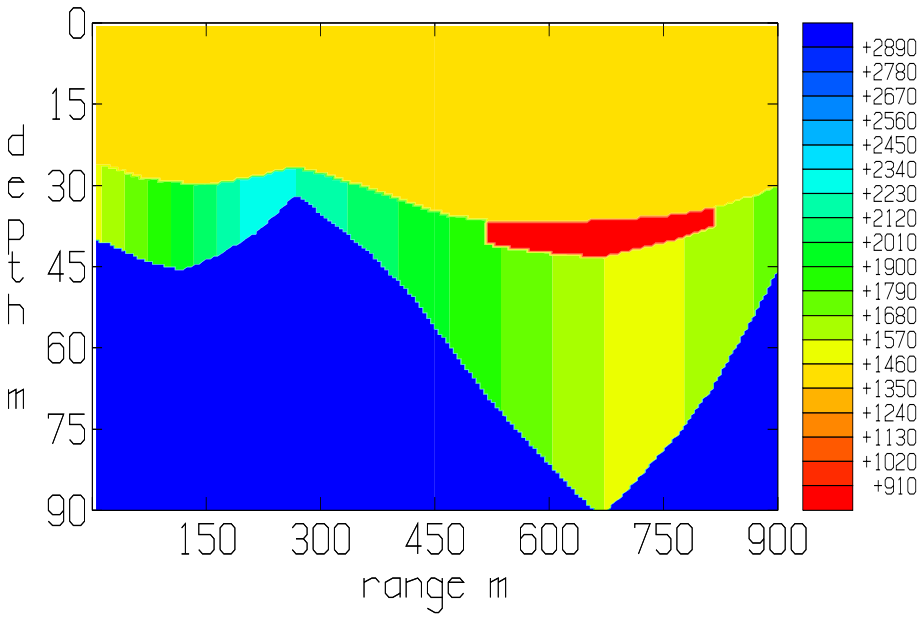

Figure 4.9: Color map of inverted velocity on a limited area.

4.3.3 Sensitivity analysis

The aim of the sensitivity analysis is to get an idea about the degree of influence of different seabed parameters on transmission loss. Of course this question is closely related to the possibility of identifying these parameters from transmission loss data. Roughly speaking, only parameters of the upper part of the sediment are expected to be of importance due to almost horizontal wave propagation. However, the actual penetration depth varies by the bathymetry, frequency and the sound velocity profile of the water. Model calculations can provide quantified information on this matter by monitoring the effect of variations of the parameters, or by computations of derivatives. The inherent problem in doing this is the choice of a relevant geophysical reference model. However, once a candidate has been found from inversion, it can be served as a point of departure of a sensitivity analysis. As an illustration we shall make a perturbation analysis of the inversion result of the previous section.

The media parameters (except for the gaspocket) are defined at five range points. The distribution of velocity, density and absorption at these points will be treated as three units, which are varied one at a time. At each of the five range points, and

independently of each other, we introduce a normally distributed perturbation around the reference value from the inversion. The standard deviation is a control variable that is stepped from zero to 100 m/s, 500 kg/m^3, 0.5 dB/λ for the velocity, density and absorption respectively. The corresponding standard deviation of the fitness function, formed as above except that measured data were replaced by the reference solution, was computed by sampling of 100 trials. The results are shown in Fig. 4.10.

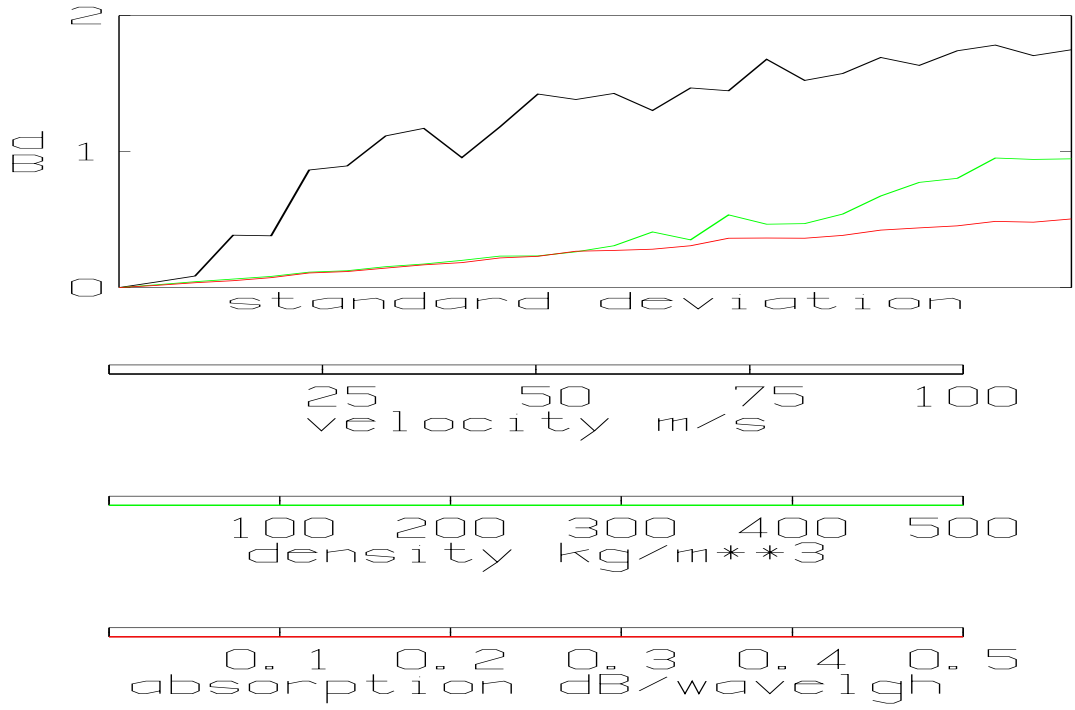

Figure 4.10: Estimated standard deviation of the fitness to the reference solution as the velocity, density and absorption are perturbed around their reference values by normal distributions of increasing rms. Each point of the curve is an estimate of the standard deviation of the fitness function from 100 trials.

We see that the velocity of the sediment greatly affects transmission loss, while the influence of the density and absorption is much less. Therefore the latter parameters will be poorly resolved by inversions from transmission loss data. It should be noted that the sensitivity curves in Fig. 4.10 are based on averaging of simulations for 75, 125, 275 and 375 Hz. A similar plot for each frequency would be somewhat different. For example, for 75 Hz the relative importance of density and absorption would be larger due to a larger penetration depth.

Sensitivity analysis indicates which parameters have a negligible influence on transmission loss. It saves computational time by simply omitting insignificant parameters from the inversion. Furthermore, it reduces the condition number of optimization methods based on gradient information, which in turn improves their performance. Alltogether it offers the perspective of doing inversions in real time. This approach was persued in [8].

4.4 Solid media inversion

The quality of the low-frequency data was low, the 35 Hz-data had too low quality to be used here and the datasets of 75 Hz, 80 Hz and 125 Hz were rather short. This reduced the chances for improvement of the already good matchings obtained above by introduction of an elastic seabed in the computational model. Nevertheless we made a try by extending the search space of the fluid media inversion 1 by the shear parameters shown in Table 4.11.

Parameter	Search interval	Number of bits
v_s^{top} [m/s]	(100, 800)	6
$\partial v_s/\partial z$ [1/s]	(-0.48, 1.92)	4
β_s [dB/λ]	(0.1, 2.0)	4

Table 4.11: The search intervals for the shear parameters in the solid inversion. The corresponding search intervals for the fluid parameters are identical to those of fluid media inversion 1 (cf. Table 4.1).

The resulting search space was large, 40 parameters (represented by 185 bits, which amounts to 4.9 $\times 10^{55}$ parameter vectors in the search space) were to be optimized by the GA. Not only the search space increases when shear parameters are introduced, also the size of the DAE-system (system of Differential Algebraic Equations) which is to be solved by JEPE-S increases. In the fluid inversions we used a vertical discretization which was adapted for the highest frequency and the largest possible thickness of each layer. By introduction of an extra transparent interface in the bedrock at depth 70 m in order to prevent gridlines to intersect each other, we got a 4-layer model (the bottommost interface is located 10 wavelengths below the transparent interface). We used 200 vertical gridpoints in the water, 250 points in the sediment, and 100 plus 200 points in the bedrock which guaranteed that we had a resolution of at least 20 points/λ for vertical waves for all frequencies in the fluid inversion. The corresponding DAE-system thus consists of 750 rows, and the coefficient matrices are tri-diagonal[5]. A corresponding resolution of the shear waves should require the following vertical discretization: 200 points in the water, 3000 points in the sediment (due to the possibility of a shear velocity of only 100 m/s), and 150 plus 400 points in the bedrock. Since we have to solve for both the compressional and shear parameters, we thus end up with a DAE-system consisting of 7300 rows and with coefficient matrices of bandwidth 11. This results in an increase of the runtime for the solid inversion by a factor of about 35. Since the runtimes of the fluid inversions on a PC-cluster consisting of 17 nodes were about three days, the corresponding solid inversion should need more than three months to produce the output.

But a resolution of 20 points/λ for waves propagating in the vertical direction is an immense overkill, that corresponds to 40 points/λ for waves propagating within the angle interval supported by the model, i.e. 30 degrees relative to the horizontal. 5 points/λ for these waves should suffice, resulting in a decrease of the DAE-system by a factor 8. We chose to use 50 points in the water, 250 points in the sediment and 20

plus 100 points in the bedrock. For the adaptive stepsize integrator we prescribed a minimum stepsize-length of $0.25 \cdot \lambda_{water}$. The GA made 27000 model runs, i.e. 108000 runs of JEPE-S in less than three days on a PC-cluster containing 19 nodes. The media parameters obtained from the inversion are shown in Figs. 4.11 and 4.12. The fitness values for the inversion data set (4 frequencies and one receiver depth (hydrophone 8)) and the control data set (6 frequencies and 7 receiver depths (hydrophones 1-7)) are shown in Tables 4.12, 4.13 and 4.14 respectively. The matching-results are very similar to the corresponding results of the fluid media inversion 1 (cf. Tables 4.2, 4.3 and 4.4). The p-velocities of Figs. 4.1 and 4.11 are also very similar. The difference in p-attenuation is compensated by the s-attenuation in Fig. 4.12. We also notice the local minimum of the shear wave velocity in the region of the surmised gaspocket between 500 and 1000 m.

Frequency	Fitness
75 Hz	2.28
125 Hz	2.52
275 Hz	2.05
375 Hz	2.25
75, 125, 275, 375 Hz	2.25

Table 4.12: Fitness values for the **inversion data set** (4 frequencies, hydrophone 8) in the solid media inversion.

Frequency	Fitness
75 Hz	4.77
80 Hz	4.52
125 Hz	2.74
275 Hz	4.12
290 Hz	5.12
375 Hz	5.73
All 6 frequencies	4.72

Table 4.13: Fitness values for the **control data set** (6 frequencies, hydrophones 1-7) in the solid media inversion when data from all receivers are matched simultaneously at each frequency.

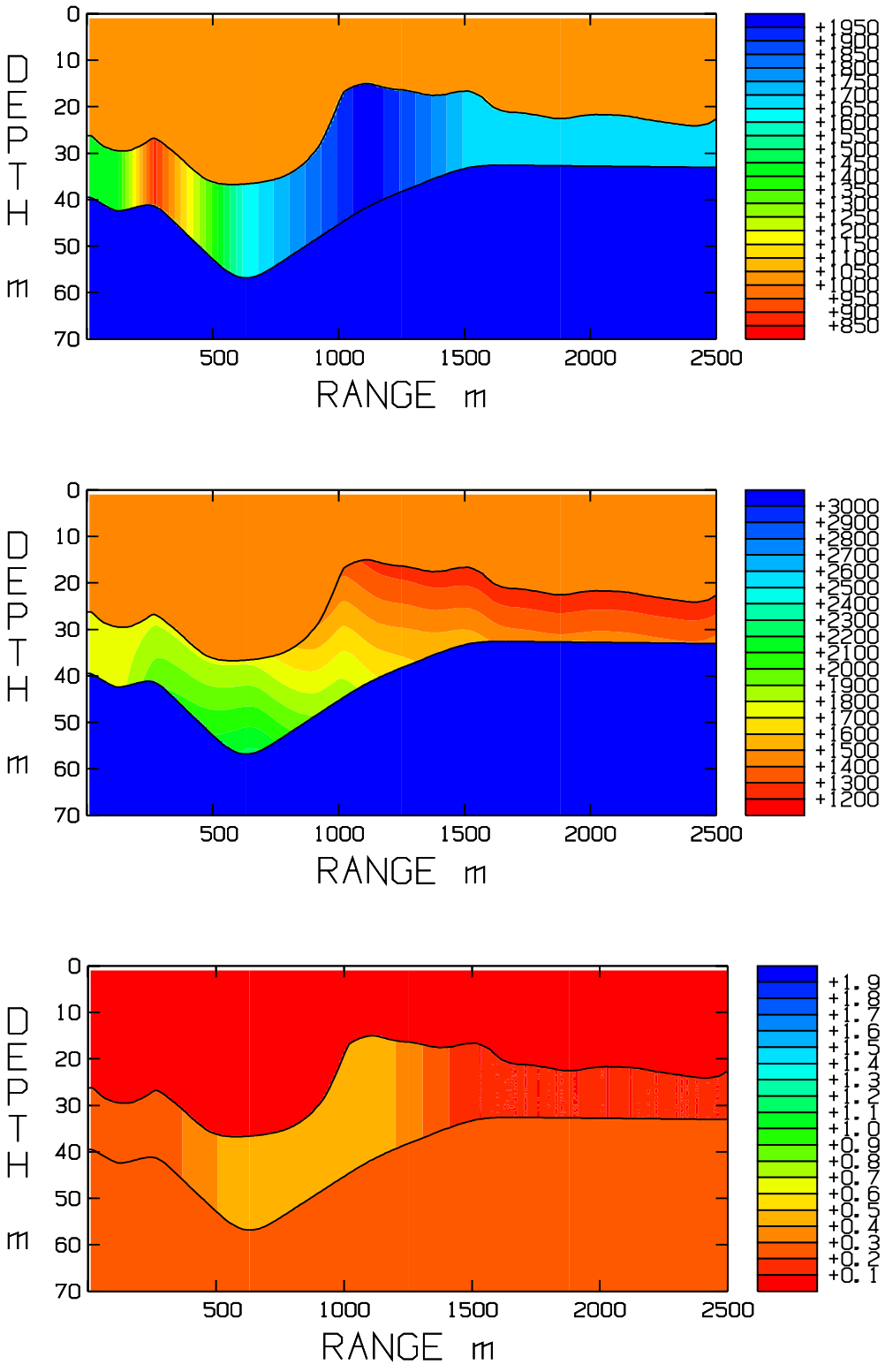

Figure 4.11: Media parameters obtained from solid media inversion: density [kg/m^3] (top), p-velocity [m/s] (middle) and p-attenuation [dB/λ] (bottom).

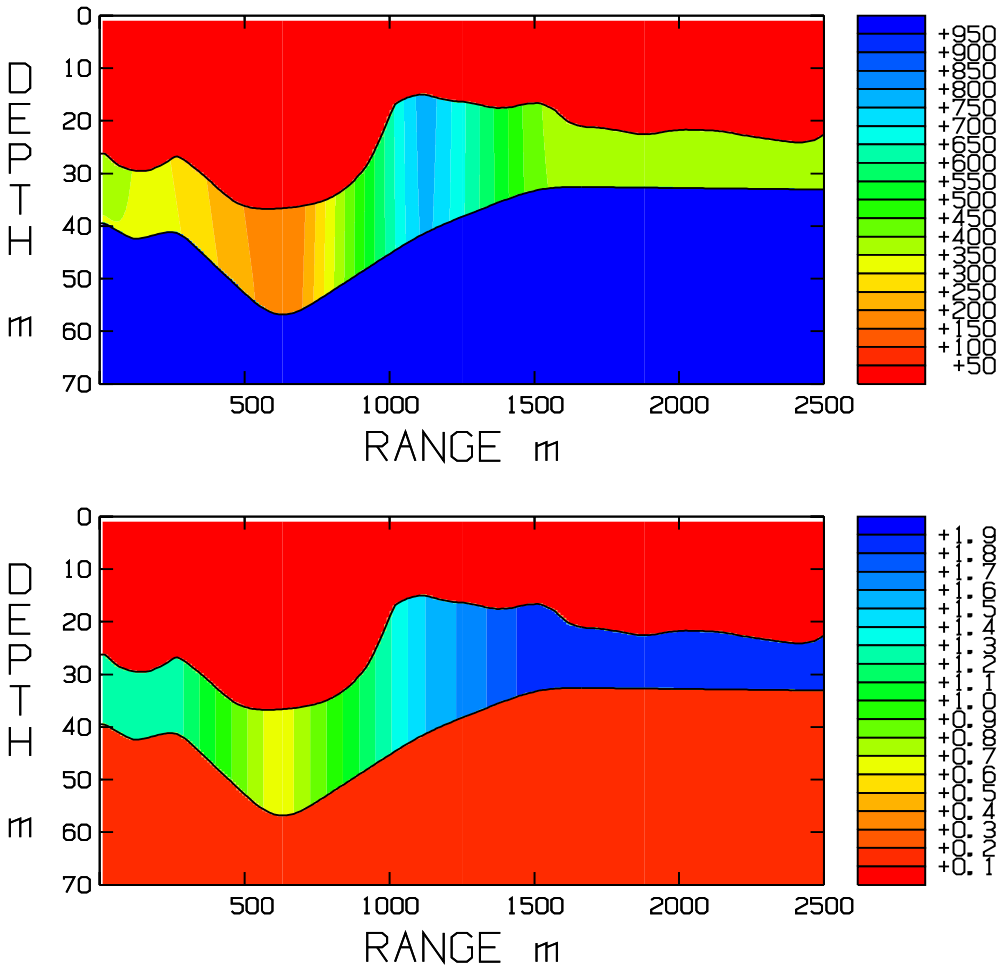

Figure 4.12: Shear parameters obtained from solid media inversion: s-velocity [m/s] (top) and s-attenuation [dB/λ] (bottom).

Frequency	Fitness
75 Hz	3.14
80 Hz	2.50
125 Hz	2.61
275 Hz	3.96
290 Hz	4.57
375 Hz	4.39
All 6 frequencies	3.88

Table 4.14: Fitness values for the **control data set** (6 frequencies, hydrophones 1-7) in the solid media inversion when data from each receiver are matched separately for each frequency.

5 Conclusions

In May 2001 a sound transmission loss experiment was carried out in a shallow bay in the southern Stockholm archipelago. The main objective of this experiment was to perform inversion in an environment within the belt of skerries which is both strongly range-dependent, and in reality is also far from 2D because of the vicinity to land. The fitness values of the inversions were quite small (2-3 dB) considering plausible errors related to both the measurements and the wave propagation model. In this sense the object of this study was well satisfied. However, a reservation must be made concerning the way the fitness function was formed due to the lack of calibrated data. Namely, the transmission loss of measured data was translated so that the average over all range points was deliberately equated to the correponding one of the simulation. It was necessary to take this measure for each combination of receiver/source because the hydrophones were not mutually calibrated. Equating the average values of measured and simulated data improves the fitness function to some degree, which is hard to assess.

Although the main interest has been to find a bottom structure that is good enough for transmission loss predictions by wave propagation models, at least some of the inverted bottom parameters should not be too far from the real ones. The most striking feature of the inversion is evidence of a large variation of the velocity of the sediment along the track. The first 500 m of the track has a hard and fast sediment, or possibly it could be so thin that the bedrock is sensed at the current frequencies. Then follows a zone over which the velocity drops by some 500 m/s and it remains quite low (1100-1200 m/s) for the last 1000 m. There is a corresponding drop of the signal strength over the transition zone to the low speed area. Due to the high noise level the low-frequency data were not possible to use at a distance larger than about 1000-1100 m. This contributes to the uncertainty of the parameter identification beyond 1200 m. The uncertainties of other inverted parameters are large. The reason is simply that they contribute much less to transmission loss according to the sensitivity analysis in Sec. 4.3.3.

The geology of the test site exhibits an appreciable variability in all directions. This poses high demands on the wave propagation model. The main difficulties are encountered in the transition zone between 500 and 1100 m. Here the water depth decreases from 37 m to 15 m and under upslope the bedrock approaches the seafloor. Prior to this, according to the geological map, there is a gassy sediment of low velocity (800 m/s). This is a rather unfavorable situation for the PE-models being used in this study. The analysis in Sec. 4.3.1 makes this evident, and the present geometry is close to the limit of applicability of a one-way propagation model. To dispense with this uncertainty we restricted the inversion to the first 900 m in Sec. 4.3.2, where the PE-model is on safe grounds. In this inversion we applied a hybrid combination of GA and the simplex method. The simplex method is a local search method and relies on a good starting approximation, which in this case was provided by inversion results from Sec. 4.1. The results on the restricted area was similar to the one obtained for the whole domain.

Three inversions were made, two with a fluid seabed model and a third with a solid

seabed. The results were consistent. A striking feature of the results was that the surmised low-impedance gaspocket between 400 and 800 m was outmanouvered by a hard and fast sediment. The reason for this is at present not well understood. It could be due to the fact that the absolute signal strengths were not accounted for in the inversions, and by this reason made it impossible for the GA to distinguish between a high impedance contrast between water and sediment caused by either a high or a low impedance respectively in the sediment. Another possible explanation could be that the bedrock under the sediment in the transition zone 500-1100 m affects the transmission loss the most, and by this reason the GA tries to find a hard and fast sediment for matching the effect of the bedrock. In contrast, an earlier FARIM-analysis of SGU-data [9] indicated a very low impedance contrast between water and sediment at the surmised gaspocket location. This was however most probably due to a thin gyttja clay layer on top of the gas-reservoir which acted as a reflector for the high frequencies used in that analysis (dominating frequencies about 7 kHz).

A notable result from the solid inversion is that the shear velocity attains its minimum at the location of the surmised gaspocket.

There are a few recommendations for future work. We need to develop good calibration techniques for low frequency transmitters and sensors [25]. It is always of interest to explore the bottom stratification at larger depths. This requires the use of lower frequencies than being used in this study. Attention must also be paid to SNR as the frequency is lowered, and how the signals can be filtered in a noisy environment.

The modelling capacity needs to be strengthened. A low-frequency Helmholtz solver suitably hybridized with a PE-solver would be beneficial for wave propagation in complicated geophysical environments. Although wave propagation models form the fundament of solving inverse problems, they need to be amended by tools for design of field experiments, optimization and sensitivity analysis.

6 Acknowledgement

We thank the following colleagues for contributions to this work:

Per Morén and Lena Frenje Lund were responsible for the transmission of the CW signals and the measurements of the sound velocity profiles onboard the test vessel HMS Urd during the field experiment in May 2001. Stefan Ban recorded the signals on land, and Lars Lekzén and Ulf Skotte provided technical support during this field work.

Mika Levonen provided MATLAB-code for conversion of the data from WAV-format to MOSES-format. Ilkka Karasalo provided routines for the data-processing. Data from the calibration of the Thomson Array were kindly made available to us by Torbjörn Ståhlsten. Per Söderberg provided valuable information about the geological milieu at the test site.

References

[1] V. Westerlin. Modelling of sound transmission loss in the baltic with a genetic algorithm. FOA report R-96-00247-2.2-SE, 1996.

[2] S. Ivansson. RPRESS, a family of computer programs for seismo-acoustic wavefields in range-independent fluid-solid media. User's guide. FOA report D-95-00169-2.2-SE, 1995.

[3] M.D. Collins. FEPE User's guide. NORDA Technical Note 365, 1988.

[4] B.L. Andersson. Analysis of transmission loss data with JEPE-S and a genetic algorithm. Methodology report FOA-R–99-01375-409–SE, 1999.

[5] B.L. Andersson. JEPE-S, a PE code for wave propagation in range-dependent fluid-solid media. Technical report FOA-R–98-00979-409–SE, 1998.

[6] J. Pihl, P. Söderberg, A. Wester, and V. Westerlin. A Method for On-site Determination of Geoacoustic Parameters. Methodology report FOA-R-99-01281-409-SE, 1999.

[7] J. Pihl and L. Abrahamsson. MODELOSS - A User Oriented Code for Transmission Loss Calculations. FOA report R-95-00173-2.2-SE, 1995.

[8] L.Abrahamsson and B.L. Andersson. Identification of seabed geoacoustic parameters from transmission loss data. Methodology report FOA-R-00-01752-409–SE, 2000.

[9] S. Ivansson, M. Levonen, and P. Söderberg. Quantitative Determination of Sediment Properties in the Baltic Using Close-Range Seismic Reflection Data. Methodology report FOA-R-00-01555-409–SE, 2000.

[10] B. Berntsen. *Model-based estimation of seafloor parameters by use of acoustic backscattering.* PhD thesis, Institutt for teleteknikk, Norwegian Univ. of Science and Technology, Trondheim, Norway, 2001.

[11] E. Larsson and L.Abrahamsson. Helmholtz and PE solutions to a benchmark problem in ocean acoustics. Dept of Scientific Computing, Uppsala University Report 210, 1998.

[12] L. Abrahamsson, L. Andersson, I. Karasalo, and A. Sundström. JEPE - a PE code for range-dependent fluid media. In *18th Scandinavium Symp. in Physical Acoustics*, pages 1–3. University of Bergen, Norway, 1995.

[13] I. Karasalo and A. Sundström. JEPE - a high-order PE-model for range-dependent fluid media. In *Proc. 3rd European Conference on Underwater Acoustics*, pages 189–194, Heraklion, Crete, Greece, 1996.

[14] A. Sundström. A stable PE model for wave propagation in fluid-solid media. Scientific report FOA-R-00-01741-409–SE, 2000.

[15] H. Maurer, D.E. Boerner, and A.Curtis. Design strategies for electromagnetic geophysical surveys. *Inverse Problems*, 16:1097–1117, 2000.

[16] M. Laumen. Newton's method for a class of optimal shape design problems. *SIAM J. Optim.*, 10:503–533, 2000.

[17] Å. Björk. *Numerical methods for least squares problems.* SIAM Philadelphia, 1996.

[18] P. Lindström and P-Å. Wedin. Methods and software for nonlinear least squares problems. Technical report UMINF-133.87, Inst. of Information Processing, University of Umeå, 1988.

[19] R.J. Urick. *Principles of underwater sound.* McGraw-Hill, 1983.

[20] A. Arnold and M. Ehrhardt. Discrete Transparent Boundary Conditions for Wide Angle Parabolic Equations in Underwater Acoustics. *J. Comput. Phys.*, 145:611–638, 1998.

[21] P. Karlsson. Transparent boundary conditions for parabolic wave equations in underwater acoustics. FOI report in preparation.

[22] B. Berntsen, I. Karasalo, M. Levonen, P. Morén, and V. Westerlin. Seabed characterization in the Baltic with the SIROB and FARIM methods. Methodology report FOA-R-99-01237-409–SE, 1999.

[23] P. Söderberg. Private communication, 2001.

[24] W.H. Press, B.P. Flannery, and W.T. Vetterling S.A. Teukolsky. *Numerical Recipes.* Cambridge University Press, 1989.

[25] L. Lekzén. Private communication, 2001.